ISSN : 0974 - 7494 Volume 8 Issue 10

Nano Science and Nano Technology
An Indian Journal

Full Paper

NSNTAIJ, 8(10), 2014 [391-400]

Investigations of nanodimers with different ring faces in contact by molecular dynamics

Jie Cheng[1]*, Jingchuan Zhu[2]
[1]College of chemical engineering, Huaqiao University, (CHINA)
[2]School of materials science and engineering, Harbin institute of technology, Harbin, (CHINA)
E-mail: t.j.cheng@163.com; chengj@hqu.edu.cn

ABSTRACT

Four nanodimers of cyclo-[(1R, 3S)-γ-Acc-D-Phe]$_3$ in contact with different ring faces as their termini in solvent $CHCl_3$ with 300, 150 and 49 molecules are modeled to investigate the two faces of cyclic peptide ring through 8 ns molecular dynamics (MD) based on Dreiding force field. The radius of monomer rings, terminal and internal sizes of dimer tubes and distances between two neighboring ring faces are analyzed. Simulation results show that the spacing in α-α dimers (dimer-II and -IV) is larger than that in γ-γ dimers (dimer-I and -III), and for dimer-IV, the time $CHCl_3$ needs to enter into its cavity is the shortest, which indicates that the channel with γ-NCH_3 termini (dimer-IV) is a good candidate carrier to absorpt $CHCl_3$.

KEYWORDS

Cyclic peptide;
Dimers;
Self-assembly;
Molecular dynamics.

INTRODUCTION

Self-assembled tubular structures have attracted much attention from the research community[1-4], because of their potential applications in biology, chemistry and materials science[5-7]. And the self-assembled cyclic peptide nanotubes (SPNs) in particular, exhibit such promising applications as specific ion sensors, nanoscale transport channels and antibacterials[8-11]

SPN are composed of cyclopeptides in which D, L-amino acids are connected alternately, and their rings adopt a quasiplanar backbone conformation with C=O and N-H groups lying approximately perpendicular to backbone plane[12]. Such a conformation facilitates the self-assembly of rings into extended hollow tubular structures by means of inter-molecular hydrogen bonds.

The existence of such a nanotube was predicted by De Santis in 1974 after he investigated the structural characteristics of liner polypeptides[13], and verified by Ghadiri and his colleagues in 1993 after they synthesized and characterized the hollow tubular structures[14]. A number of subsequent investigations reported their syntheses, characteristics and specific functional applications[10,15-19]. The work involved needle-shaped microcrystals as large as 200μm, prepositioned dimers crystals, self-assembly embedded in the lipid bilayers and so on[19-20].

The properties of inner and outer surfaces of the peptide nanotube can be modified by choosing different amino acid residues, and the ring size of the peptide nanotube can be adjusted by changing the numbers of peptide subunits employed. Inspired by the remarkable functional structures, more and more investigators devoted their efforts to investigate the microscopic struc-

tures of self-assembled cyclic peptide nanotubes[21-22]; some theoretical studies by ab initio, semiempirical approaches and molecular dynamics (MD) have also been performed[23-25], which have thrown light on the structures of these nanotubes and their applications[26-27].

These work focused on whether cyclic peptide rings prefer parallel or antiparallel inter-ring stack formation from the energy standpoint[24], the difference in the interaction between two ring faces was not known until Manuel Amorin et al designed a hybrid system of α-γ cyclic peptide which consists of alternating (1R, 3S)-3-aminocyclohexanecarboxylic acid (γ-Acc-OH) and D-α-amino acid. One ring surface of it is positioned by C=O and N-H groups of γ amino acid (γ-face) and the other residue surface is positioned by C=O and N-H groups of α amino acid (α-face). Manuel Amorin et al synthesized and characterized two kinds of tubelets with the stacking of more than two rings blocked by N-methylation of either α amino acid (for formation of γ-γ bound tubelets) or γ-amino acid (for formation of α-α bound tubelets), and they verified that α-α interaction is more stable than γ-γ interaction by NMR[28-30].

However, it is difficult to observe experimentally the detailed topological structure of two ring faces and the influence of ring faces on the nanotube properties is not well understood. Molecular dynamics (MD) simulation provides a microscopic picture of such phenomena at atomistic level. Therefore, in the present study, we studied two ring faces by modeling four dimer self-assemblies from cyclo-[(1R, 3S)-γ-Acc-D-Phe]$_3$ in $CHCl_3$ solvent. The detailed topological conformations of ring faces are compared by analyzing the H-bonds between inter-rings, dimer volumes, terminal and internal sizes of dimer tube and binding energies of $CHCl_3$ in dimer cavities. The results show that the dimers with different ring faces as the ends exhibit different ability to absorp of $CHCl_3$ into their cavities. This provides a way to design new cyclic peptide transport channel.

MODELS AND MODELING METHODS

Single dimer model

The two ring faces of cyclo-[(1R, 3S)-γ-Acc-D-

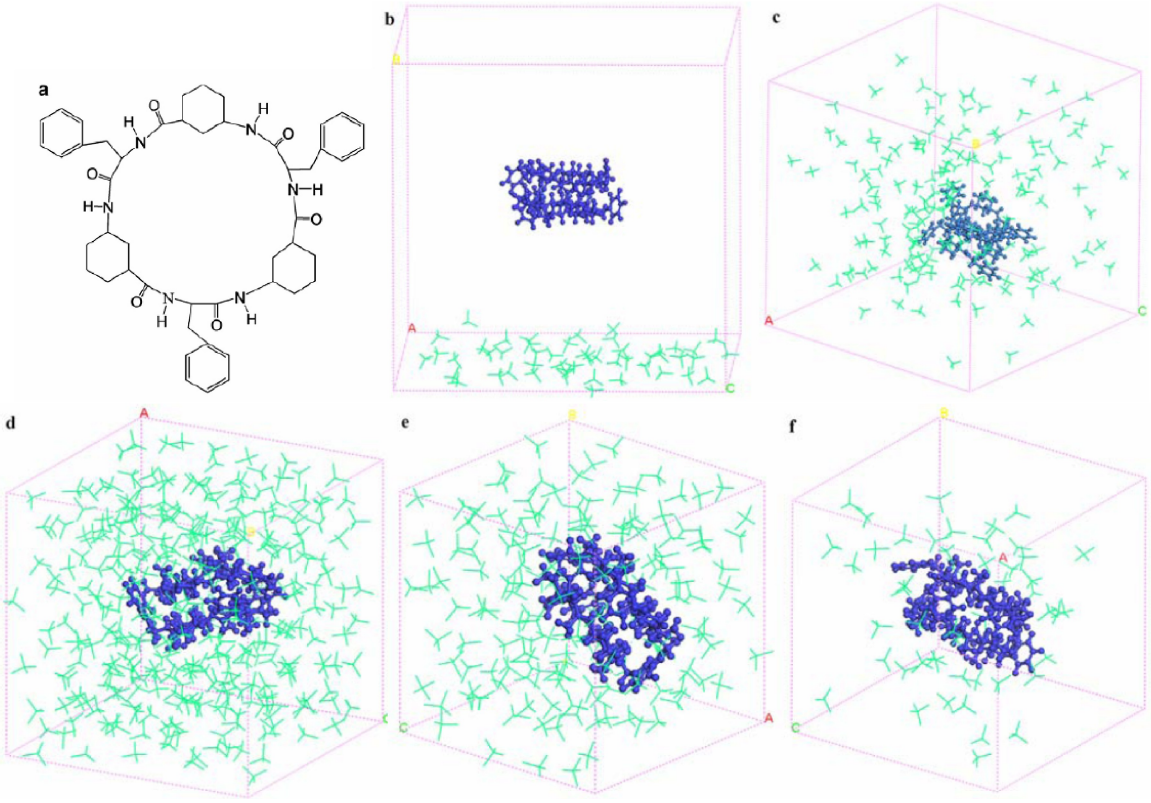

Figure 1 : Scheme of cyclo-[(1R, 3S)-γ-Acc-D-Phe]$_3$ (a) and solvent dimer models. (b)Initial solvent model with dimer separate from $CHCl_3$ molecules. (c)Initial solvent model with solvent molecules around the dimmer and filled the box. Initial configuration used for 8 ns MD (d)in model-I (300 $CHCl_3$), (e)in model-II (150 $CHCl_3$) and (f) in model-III (49 $CHCl_3$).

Phe]$_3$ (Figure 1a) positioned by N-H and C=O groups of α- and γ-amino acid residues respectively are different due to steric and polarity difference of amino acid residues[28]. In addition, it is found through experimental and theoretical studies that cyclic peptide rings prefer an antiparallel arrangement[23,31]. It was assumed that nanotubes with different ring faces at the termini have two types of channels: one with α-NH as its ends and the other with γ-NH as its ends. But they all have hydrophilic termini. If hydrogens are directly connected to the nitrogens of channel terminal faces are substituted by methyls, there are another two types of channels: one with α-NCH_3 as its ends and the other with γ-NCH_3 as its ends. But they all have hydrophobic termini. These four types of channels are different in structures and properties.

We built four dimers to represent four types of channel structures: dimer-I possess α-NH termini in contact with γ-faces, dimer-II possesses γ-NH termini in contact with α-faces, dimer-III possesses α-NCH_3 termini in contact with γ-faces, and dimer-IV possesses γ-NCH_3 termini in contact with α-faces. Single dimers are optimized by MM firstly, and the convergence criterion is 0.00001 kcal/mol rms gradient. As shown in Figure 1, Dimer-I and dimer-III represent γ-γ interactions, while dimer-II and -IV represent α-α interactions; dimer-I and -II have hydrophilic termini (Figure 1b and c) and dimer-III and -IV have hydrophobic termini (Figure 1d and e). It has some structures and properties of a longer channel although as the foundational unit of antiparallel nanotube a dimer is short.

Solvent dimer model

In order to investigate the structure and property of dimers in solvent, three solvent models are built by putting the four dimers built separately into solvent boxes filled with 300 (model-I), 150 (model-II) and 49 (model-III) $CHCl_3$ molecules. The models were built using the following two methods: 1) the initial position of dimer and $CHCl_3$ molecules are separate as shown in Figure 1b; 2) the solvent molecules distribute around and fill the box as shown in Figure 1c. The initial lattice parameters are $a=b=c=50$ Å and $\alpha=\beta=\gamma=90°$.

150 ps MD was used to obtain equilibrium density and lattice parameters of model-I and model-II. A NPT ensemble at 298 K, a time step of 1fs and a nose thermostat[32] were employed during MD. Ewald method was used to calculate the long-range interactions with an accuracy of 0.001 kcal/mol and an updated width of 3 Å. After 50 ps, the system reaches equilibrium. The equilibrium density of both model-I and model-II is 1.65g/cm^3, and the equilibrated lattice parameters in model-I are $a=b=c=32.12$ Å as shown in Figure 1d and the lattice parameters in model-II are $a=b=c=25.91$ Å as shown in Figure 1e.

Because there are only 49 $CHCl_3$ molecules in model-III, 150 ps MD with A NVT ensemble was use to enable the dimer and solvent molecules to reach equi-

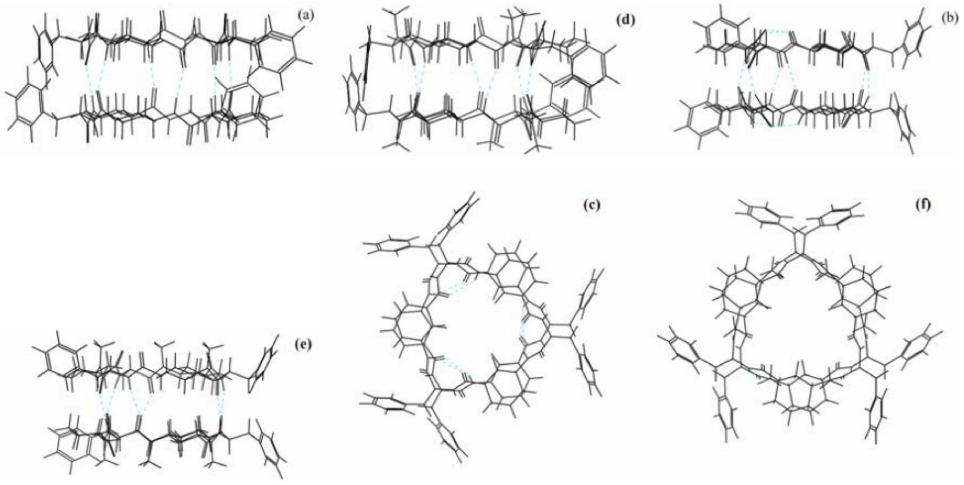

Figure 2 : Four single dimers. (a) Dimer-I with α-NH termini in contact with γ-faces. (b) Dimer-II with γ-NH termini in contact with α-faces. (c) Top view of dimer-II. Three intra-molecular H-bonds at termini, make the dimer look like a cage. (d) Dimer-III with α-NCH_3 termini in contact with γ-faces. (e) Dimer-IV with γ-NCH_3 termini in contact with α-faces, and (f) top view of dimer-IV. Dimer-I and -III representing γ-γ interactions, and dimer-II and -IV representing α-α interactions

librium, while other MD conditions are the same as what are mentioned above. At the end of MD, solvent molecules embraced the dimer as shown in Figure 1f. In order to be able to compare model-III with model-I and model-II to make the analysis easier, the lattice parameters are set to $a=b=c=30$ Å (between those of model-I and model-II).

MD simulation of 8 ns was performed with solvent model-I, model-II and model-III, and two initial models of each solvent model were used to get consistent results. NVT ensemble is employed with a time step of 1fs at 298 K, and a nose thermostat was employed to keep the system temperature constant during MD. Ewald method was used to calculate the long-range interactions with an accuracy of 0.001 kcal/mol and an updated width of 3 Å. For every 1000 fs, the molecular structure was stored in the trajectory file for analysis. In the whole MD simulation process, lattice angles are constrained at $\alpha=\beta=\gamma=90°$ to make the analysis easy and some $CHCl_3$ molecules which entered the dimer cavities during NPT MD are deleted for consistence.

All the modeling work is conducted with Materials Studio software (Accelrys Inc.) on sgi3800 origin sever. The MD calculations are all based on the COMPASS force field, which is an *ab initio* force field, and consists of bonding and nonbonding terms. The bonding terms include stretching, bending, and torsion energies as well as the diagonal and off-diagonal cross-coupling terms. COMPASS is usually used to realize accurate and simultaneous prediction of gas-phase properties and condensed-phase properties for a broad range of small molecules and polymers[33-35].

RESULTS AND DISCUSSION

Structure of dimers

Single dimers

It can be seen from Figure 2 that the side chain benzyls tilt to γ-face, and dimer-I and -III are enclosed by group's benzyl. In dimer-II and -IV, the hydrophilic groups N-H and C=O of residue γ-Acc are repulsed to the inner tube slightly by the phenyl of hydrophobic groups, and there are six intra-molecular H-bonds formed at the ends of dimer-II, which looks like a cage as shown in Figure 2c and d. This result is consistent with the results of Amorin's, who also observed a cage-like dimer through experiment[30].

The hydrogen-bonding distance (N-O) between neighboring peptide rings is in the range of 2.773 Å ~3.004 Å, and the distance between neighboring peptide rings (measured from the nearest two carbons of methylene moieties of each cyclohexane projecting into the inner tube) is in the range of 4.805-4.864 Å. The hydrogen-bonding distance (N-O) and the distance of neighboring peptide rings Amorin[28] measured are in the range of 2.7-2.9 Å and 4.85-4.90 Å respectively, and that of Rebeca Garcia-Fandino[36-37] calculated are in range of 2.9-3.0 Å and 4.8-5.0 Å respectively. The very good agreement between experimental results indicates that COMPASS force field fits our system.

Dimers in solvent

There is no interaction between dimers in the three models, because the minimum lattice of three models is that of model-II (25 Å), which is beyond the sum distance of dimer diameter (18 Å) and the cutoff distance of Ewald (6 Å), so the dimers can interact only with solvent molecules. In addition, in model-I and model-II, the dimers are immersed in the solvent completely for the solvent with equilibrium density embraces the dimers. So we can only investigate the interactions of one dimer and solvent molecules, and this saves much computation time. In model-III, the dimers interact only with solvent molecules because the solvent molecules form aggregate around the dimers. Although there is some vacuum in the box, it can make the box large enough to eliminate the dimer interacting with dimers in other cell. This makes the analysis easy.

In order to verify the consistence of results, we repeated MD several times and obtained the same results from different initial models.

Stability of dimers

Information derived from MD trajectories is meaningful only at equilibrium, and so there are two criteria to determine whether the system reached equilibrium: one is energy and the other is temperature. During our simulation test, the energy and temperature have rapidly reached equilibrium at about 500 ps. The energy varies in a range of -190~-160 kcal/mol, and the temperature varies in a range of 260~305 K.

At the end of 8 ns MD simulation, the four dimers

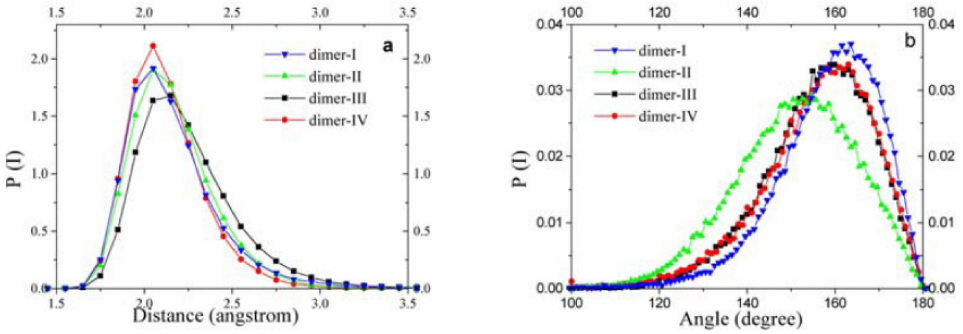

Figure 3 : Statistical distribution of (a) distances and (b) angles of inter-ring H-bonds in four dimers during 8 ns MD. All the distances and angles are within the usual variation limits of H-bonds

are all stable in three solvent models. As shown in Figure 3, the statistical distributions of distances of H-bonds (H…O) range from 1.5 Å to 3.2 Å, the maximum distribution of distance is 2.0 Å; the H-bonding angles (∠N-H…O) range from 120 to 180 degree, the maximum distribution is within the range of 150-170 degree. All the distances and angles are within the range of usual variation limits of H-bonds, which suggest these hydrogen bonds are strong enough to stack the peptide rings during 8 ns simulation.

The stability of dimers corresponds to the experimental results of Amorin, which proves the existence of α-α and γ-γ dimers. Amorin et al characterized α-α and γ-γ hydrogen bonds by NMR and FT-IR, and synthesized and characterized prismatic crystals α-α and γ-γ dimers in an antiparallel β-sheet linked by inter molecular hydrogen bonds using X-ray diffractometry[28,29].

In addition, considering dimer-I and -II are stable in solvent, and they also have free donors and acceptors of hydrogen bonds at their both terminal ends, they are expected to stretch into longer nanotubes, which can be used as transport channels[37,38].

Adsorption of dimers

At the end of 8 ns MD simulation, the lumina of three dimers exhibit its ability to adsorb $CHCl_3$, and there is no $CHCl_3$ in dimer-II. As shown in TABLE 1, the dimer-IV in three models takes the shortest time (38 ps in model-III) to adsorb $CHCl_3$ molecule into its cavity. This agrees well to the results of Amorin[28], who characterized the $CHCl_3$ molecule in the dimer-IV cavity for the first time. Dimer-I takes longer (255 ps in model-III) and dimer-III takes quite a long time (6232 ps in model-III). In order to get consistent results, we performed several runs on each initial configuration. Every

TABLE 1 : Time needed for $CHCl_3$ molecule to enter dimer cavity

	dimer-I	dimer-II	dimer-III	dimer-IV
49 $CHCl_3$	255 ps	-	6232 ps	38 ps
150 $CHCl_3$	51 ps	-	178 ps	14 ps
300 $CHCl_3$	45 ps	-	160 ps	6 ps

time $CHCl_3$ molecules need similar time to enter the cavity of a dimer. So we think the characteristic time for solvent molecules to enter the dimer interface reflects the ability of dimers to absorb $CHCl_3$ molecules into its cavity to some extent.

In addition, it is noticed that with the increase of the number of solvent molecules, the time for $CHCl_3$ to enter the dimer cavities decreases. But the order of time for $CHCl_3$ to enter the dimer cavities remains unchanged. So it can be concluded that the number of solvent $CHCl_3$ molecules do not change the absorption property of dimers. The channel with γ-NCH_3 termini has the best absorption.

In order to see better the detailed topological structure of four dimers and the factors having influences on the dimers' absorption properties, we analyzed the spacing of dimers and binding energies of $CHCl_3$ in dimer in model-III in the following sections. Model-III is analyzed because there are less solvent molecules which not only reduce the calculating time but also show the interactions of dimers and $CHCl_3$ molecules better.

Spacing of dimers

The steric conformation and polarity of amino acid residues have their effect on the volume of dimers, which provides accommodation for $CHCl_3$ to reside. The distances between two mass centers of monomer rings and van der waals radius of rings reflect the volumes of dimers.

Full Paper

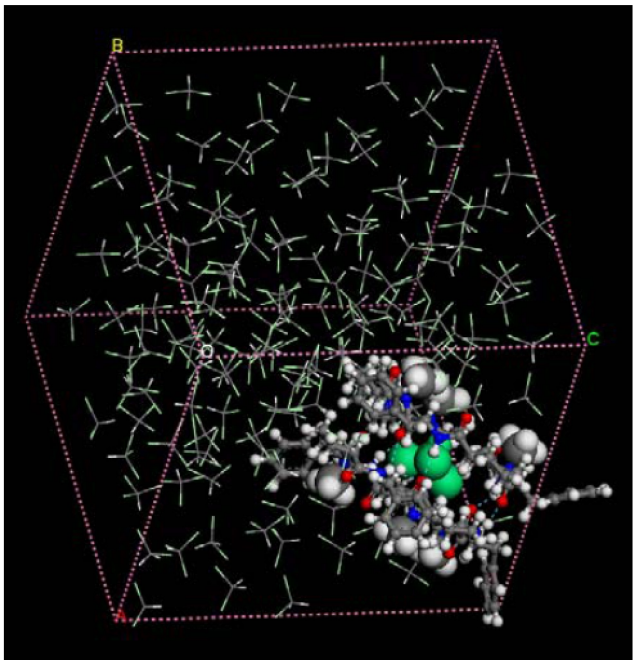

Figure 4 : Snapshots of dimer-IV in model-III during MD simulation. The lines represent $CHCl_3$ molecules, stick and ball represent cyclic peptide dimers and green CPKs represent the $CHCl_3$ molecules in dimer cavity

Distances N…O of hydrogen bonds

The N…O average distances during 8 ns are shown in. It can be seen from TABLE 2 that the distance in dimer-I and dimer-III (γ-γ dimer) are 3.11 Å and 3.18 Å, while the distance in dimer-II and dimer-IV (α-α dimer) are 3.01 Å and 3.02 Å respectively. As shown in Figure 5, the variations of N…O distances during MD simulation, α-α hydrogen bonds (dimer-I and -III) varies in a range of 2.9~3.1 Å and the N…O distances of γ-γ hydrogen-bonds (dimer-II and -IV) varies in a range of 3.0~3.2 Å mainly.

TABLE 2 : Distances N…O of hydrogen bonds

	dimer-I	dimer-II	dimer-III	dimer-IV
Average distance (Å)	3.11	3.02	3.18	3.01

In general, the strength of H-bond increases with its length. The experimental and calculating results have shown that α-α dimer is more stable than γ-γ dimer by the geometries of the CO···HN moieties, electron densities and NMR signals[28-29,36]. Our findings are complement to the reliability of their results. We obtained the O…N distances in α-α hydrogen bonds from calculations is 0.1 Å shorter than that of γ-γ hydrogen bonds, which indicates the hydrogen-bond alignment in the α-α pattern is preferred than that in the γ-γ pattern.

Distances between neighboring rings

It can be seen from Figure 6 that the distances between neighboring rings in dimer-I and -III vary in a range of 4.0~4.4 Å, dimer-II in a range of 5.0~5.4 Å and dimer-IV in a range of 5.5~5.9 Å. In general, the distances between adjacent nanotube rings determined experimentally by X-ray diffraction is 4.7-4.8 Å[16], and those calculated by Rebeca Garcia-Fandino are about 4.8-5.0 Å[37], similar to other CP dimers[24, 39]. The observed values experimentally in nanotubes are slightly longer than those computed may attribute to a synergetic effect that enhances the interaction energies between monomers[40]. While in our simulation results, the spacing in dimers with α-faces in contact (dimer-II and -IV) is larger than that with γ-faces in contact (dimer-I

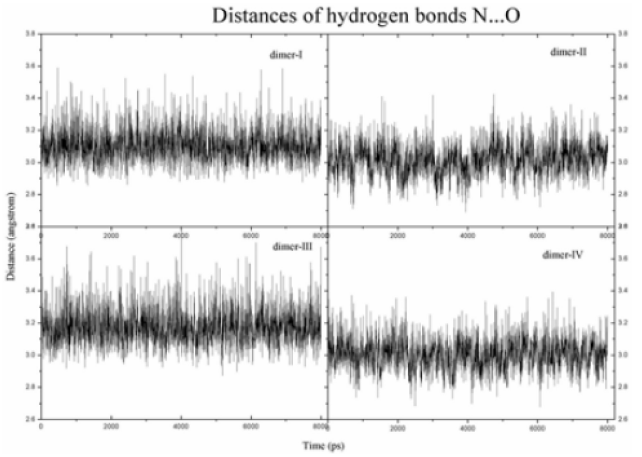

Figure 5 : Changes of hydrogen bonds N…O during simulation. γ-γ hydrogen bonds vibrating in a wider range and distances of α-α hydrogen-bonds are shorter than that of γ-γ hydrogen-bonds

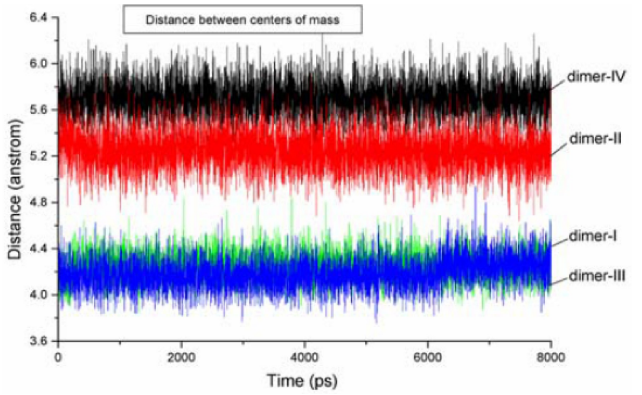

Figure 6 : Distance between two centroids of monomer rings. Distances in dimers with α-faces in contact (dimer-II and -IV) are longer than that with γ-faces in contact (dimer-I and -III)

and -III). This may attribute to the effect of solvent molecules. Moreover, in α-α dimers, the distance of dimer-IV is larger than that of dimer-II, which indicates that dimer-IV is more easily polarized by solvent $CHCl_3$ molecules and it can therefore provide $CHCl_3$ molecules with more room, and so, $CHCl_3$ molecules can more easily enter.

In addition, the distances between two neighboring rings in the four dimers have little changes during MD simulation, which also indicates the nanotubes remain stable in solvent $CHCl_3$.

Van der waals radii of rings

As shown in Figure 7, the curves of monomer radius in dimer-I vary in a range of 2.6~3.0 Å before 255ps and vary in a range of 2.7~3.1 Å after 255ps in dimer-I. The curves of dimer-II vary in a range of 2.3~2.7 Å from beginning to end during MD simulation. In dimer-III, the curves vibrate in range of 2.5~2.9 Å before 6232 ps and vary in a range of 2.6~3.0 Å after 6232 ps. The curves of dimer-IV vary in a range of 2.7~3.1 Å and they only decline slightly during the last 1000ps. The distance is measured from the mass center of a monomer to the nearest hydrogen atom of hexamethylene. The radius with $CHCl_3$ in dimer cavity are corresponding to that of Amorin, they measured the cyclindical dimer-IV an approximate van der Waals internal diameter of 5.4 Å, which is filled with one molecule of chloroform[28].

It can be seen from Figure 7 that radius of dimer-II is relatively smaller than those of others, so it is difficult for $CHCl_3$ to enter into its cavity, the $CHCl_3$ molecules can enlarge the monomer rings for dimer-I and -III after they enter the dimers. For dimer-IV, its radius is large enough, and so, it needs the shortest time to adsorb $CHCl_3$.

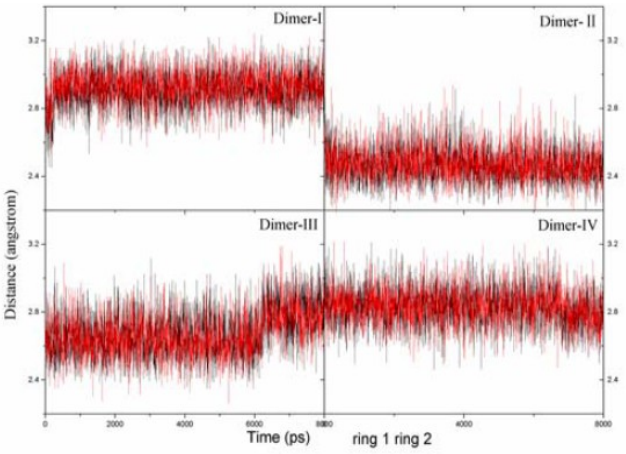

Figure 7 : Van der waals radii of monomer rings

Sizes of terminal and internal dimer tubes

As shown in Figure 8, the internal and terminal sizes in the four solvent models are compared, by measuring distances between hydrogen atoms or carbon atoms of methyl which connected directly to the nitrogen for convenience. In dimer-I and -IV, the sizes of internal and terminal tube both vibrate about 4.5 Å, and the consistence of internal and terminal sizes facilitate the entry of $CHCl_3$ into the dimer. In dimer-III, the radius of terminal tube is larger than that of internal tube and the sizes of internal and terminal tubes vibrate at 5.3 and 4.0 Å respectively during 0~6232 ps before $CHCl_3$ molecule enter its cavity. After $CHCl_3$ enter the cavity of a dimer, the differences in distance between internal and terminal sizes are reduced under the attraction of $CHCl_3$

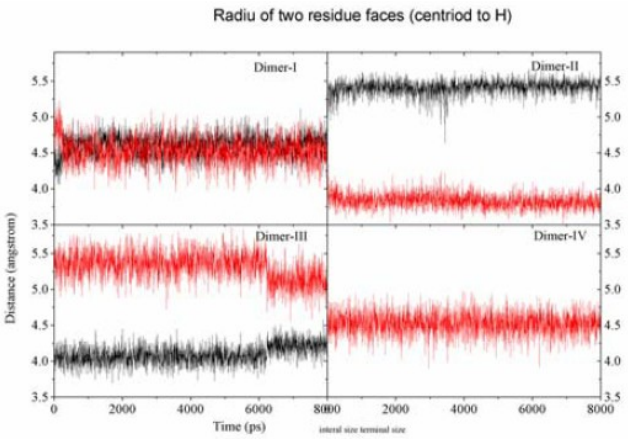

Figure 8 : Sizes of terminal and internal dimer tubes

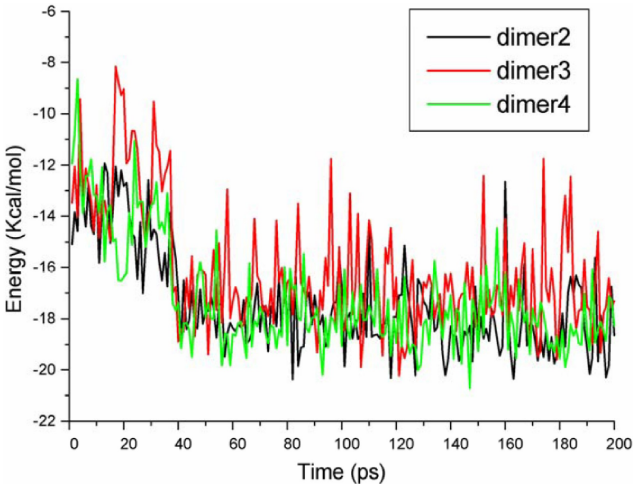

Figure 9 : Binding energies of $CHCl_3$ in cavities of dimer-I, dimer-III and dimer-IV for 200 ps

molecule, while the terminal size is still larger than the internal size. As for dimer-II, six intra-molecular hydrogen bonds formed at the ends of the dimer make the terminal size very small, $CHCl_3$ is thus prevented from entering the cavity of a dimer.

It can be seen from the discussions above that the sizes of terminal and internal dimers play a key role in preventing $CHCl_3$ from entering the cavity of a dimer.

Binding energies of $CHCl_3$ in dimer

Binding energy E_{bind} is calculated using $E_{bind} = E_{tot} - (E_{nanotube} + E_{solvent})$, where $E_{solvent}$ is the potential energy of the $CHCl_3$ molecule adsorbed in the nanotube, and $E_{nanotube}$ is the potential energy of the nanotube.

As shown in Figure 9, there is no evident difference in the three energy curves, which indicate there is no difference in energy potential barriers for $CHCl_3$ to enter the three dimers. So, it can be concluded that the geometry of a dimer plays a key role in absorbing $CHCl_3$

CONCLUSION

It can be seen from the results of molecular dynamics simulation conducted with four dimers of cyclo-[(1R, 3S)-γ-Acc-D-Phe]$_3$ in solvent $CHCl_3$ with 300, 150 and 49 molecules to investigate their structural characters and absorbing properties, that due to the steric structure and polarity of α- and γ-amino acid, the volumes of dimers, sizes of terminal and internal dimers in the four dimers are different, the spacing in α-α dimers (dimer-II and -IV) is larger than that in γ-γ dimer (dimer-I and -III), and dimer-IV have the largest volume. In the four dimers, dimer-II can not absorb $CHCl_3$ due to the intra-molecular H-bond formed at the termini, dimer-I needs longer time to absorb $CHCl_3$, dimer-III needs quite long time to absorb $CHCl_3$, and dimer-IV needs the shortest time to absorb $CHCl_3$. Thus the channel with γ-NCH_3 termini is a good candidate for absorption of $CHCl_3$. It is one of the ways to design a new cyclic peptide channel to select a different ring face as the terminus of a cyclic peptide.

ACKNOWLEDGE

This work was supported by Program of Excellent Team at Harbin Institute of Technology

REFERENCES

[1] G.M.Whitesides, J.P.Mathias, C.T.Seto; Molecular Self-Assembly and Nanochemistry - A Chemical Strategy for the Synthesis of Nanostructures. Science, **254**, 1312-1319 **(1991)**.

[2] H.J.Jong, S.Toshimi, S.Seiji; Self-assembling structures of steroidal derivatives in organic solvents and their sol–gel transcription into double-walled transition-metal oxide nanotubes. J.Mater.Chem., **15**, 3979-3986 **(2005)**.

[3] A.Janshoff, K.P.Dancil, C.Steinem, D.P.Greiner, V.S.Y.Lin, C.Gurtner, K.Motesharei, M.J.Sailor, M.R.Ghadiri; Macroporous p-type silicon Fabry-Perot layers. Fabrication, characterization, and applications in biosensing, J.Am.Chem.Soc., **120**, 12108-12116 **(1998)**.

[4] M.R.Ghadiri, K.Kobayashi, J.R.Granja, R.K.Chadha, D.E.McRee; The Structure and Thermodynamic Basis for the Formation of Self-Assembled Peptide Nanotubes. Angew.Chem.Int.Ed.Engl., **34**, 93-95 **(1995)**.

[5] S.Fernandez-Lopez, H.S.Kim, E.C.Choi, M.Delgado, J.R.Granja, A.Khasanov, K.Kraehenbuehl, G.Long, D.A.Weinberger, K.M.Wilcoxen, M.R.Ghadiri; Antibacterial agents based on the cyclic D,L-alpha-peptide architecture. Nature, **412**, 452-455 **(2001)**.

[6] H.Rapaport, H.S.Kim, K.Kjaer, P.B.Howes, S.Cohen, J.Als-Nielsen, M.R.Ghadiri, L.Leiserowitz, M.Lahav; Crystalline cyclic peptide nanotubes at interfaces. J.Am.Chem.Soc., **121**, 1186-1191 **(1999)**.

[7] J.S.Quesada, M.P.Isler, M.R.Ghadiri; Modulating Ion Channel Properties of Transmembrane Peptide Nanotubes through Heteromeric Supramolecular Assemblies. J.Am.Chem.Soc., **124**, 10004-10005 **(2002)**.

[8] J.Sanchez-Quesada, M.R.Ghadiri, H.Bayley, O.Braha; Cyclic peptides as molecular adapters for a pore-forming protein. J.Am.Chem.Soc., **122**,11757-11766 **(2000)**.

[9] T.D.Clark, L.K.Buehler, M.R.Ghadiri; Self-assembling cyclic beta(3)-peptide nanotubes as artificial transmembrane ion channels. J.Am.Chem.Soc., **120**, 651-656 **(1998)**.

[10] W.S.Horne, N.Ashkenasy, M.R.Ghadiri; Modulating charge transfer through cyclic D,L-alpha-peptide self-assembly.Chem.Eur.J., **11**, 1137-1144 **(2005)**.

[11] L.Motiei, S.Rahimipour, D.A.Thayer, C.Wong, M.R.Ghadiri; Antibacterial cyclic DL-alpha-glycopeptides.Chem.Commun., 3693-3695 **(2009)**.

[12] J.R.Granja, J.D.Hartgerink, M.R.Ghadiri, R.A.Milligan, D.E.McRee; Self-Assembling Organic Nanotubes. Abstracts of Papers of the American Chemical Society, **207,** 488-ORGN **(1994)**.

[13] P.D.Santis, S.Morosetti, R.Rizzo; Conformational Analysis of Regular Enantiomeric Sequences, Macromolecules, **7**, 52-58 **(1974)**.

[14] M.R.Ghadiri, J.R.Granja, R.A.Milligan, D.E.McRee, N.Khazanovich; Self-assembling organic nanotubes based on a cyclic peptide architecture, Nature, **366**, 324-327 **(1993)**.

[15] M.R.Ghadiri, J.R.Granja, L.K.Buehler; Artificial transmembrane channels from self-assembling peptide nanotubes, Nature, **369**, 301-304 **(1994)**.

[16] J.D.Hartgerink, J.R.Granja, R.A.Milligan, M.R.Ghadiri ; Self-assembling peptide nanotubes. J.Am.Chem.Soc., **118**, 43-50 **(1996)**.

[17] N.Khazanovich, J.R.Granja, D.E.McRee, R.A.Milligan, M.R.Ghadiri ; Nanoscale Tubular Ensembles with Specified Internal Diameters-Design of A Self-Assembled Nanotube with A 13-Angstrom Pore. J.Am.Chem.Soc., **116**, 6011-6012 **(1994)**.

[18] T.D.Clark, J.M.Buriak, K.Kobayashi, M.P.Isler, D.E.McRee, M.R.Ghadiri; Cylindrical beta-sheet peptide assemblies, J.Am.Chem.Soc., **120**, 8949-8962 **(1998)**.

[19] K.Motesharei, M.R.Ghadiri; Diffusion-limited size-selective ion sensing based on SAM-supported peptide nanotubes. J.Am.Chem.Soc., **119**, 11306–11312 **(1997)**.

[20] D.T.Bong, T.D.Clark, J.R.Granja, M.R.Ghadiri; Self-assembling organic nanotubes. Angew.Chem.Int.Ed.Engl., **40**, 988-1011**(2001)**.

[21] M.Engels, D.Bashford, M.R.Ghadiri; Structure and dynamics of self-assembling peptide nanotubes and the channel-mediated water organization and self-diffusion. a molecular dynamics study. J.Am.Chem.Soc., **117**, 9151-9158 **(1995)**.

[22] E.Khurana, S.O.Nielsen, B.Ensing, M.L.Klein; Self-Assembling Cyclic Peptides:. Molecular Dynamics Studies of Dimers in Polar and Nonpolar Solvents. J.Phys.Chem.B., **110**, 18965-18972 **(2006)**.

[23] J.P.Lewis, N.H.Pawley, O.F.Sankey; Theoretical investigation of the cyclic peptide system cyclo[(D-Ala-Glu-D-Ala-Gln)$_{(m=1-4)}$]. J.Phys.Chem.B., **101**, 10576-10583 **(1997)**.

[24] G.J.Chen, S.Su, R.Z.Liu; Theoretical Studies of Monomer and Dimer of Cyclo(L-Phe^{1}-D-Ala^{2})$_n$] and Cyclo[(-L-Phe^{1}-D-^{Me}N-Ala^{2})$_n$]$_{(n=3-6)}$. J.Phys.Chem. B., **106**, 1570-1575 **(2002)**.

[25] R.A.Jishi, R.M.Flores, M.Valderrama, L.Lou, J.Bragin; Equilibrium geometry and properties of cyclo[(Gly-D-Ala)$_4$] and {cyclo[(Gly-D-Ala)$_4$]}$_2$ from density functional theory. J.Phys.Chem.A., **102**, 9858-9862 **(1998)**.

[26] H.S.Kim, J.D.Hartgerink, M.R.Ghadiri; Oriented self-assembly of cyclic peptide nanotubes in lipid membranes. J.Am.Chem.Soc., **120**, 4417-4424 **(1998)**.

[27] M.Tarek, B.Maigret, C.Chipot; Molecular dynamics investigation of an oriented cyclic peptide nanotube in DMPC bilayers.Biophys.J., **85**, 2287-2298 **(2003)**.

[28] M.Amorin, L.Castedo, J.R.Granja; New cyclic peptide assemblies with hydrophobic cavities: The Structural and Thermodynamic Basis of a New Class of Peptide Nanotubes, J.Am.Chem.Soc.,**125**, 2844-2845 **(2003)**.

[29] M.Amorin, L.Castedo, J.R.Granja; Self-assembled peptide tubelets with 7 angstrom pores.Chem.Eur.J., **11**, 6543-6551 **(2005)**.

[30] R.J.Brea, M.Amorin, L.Castedo, J.R.Granja; Methyl-blocked dimeric α,γ-peptide nanotube segments: Formation of a peptide heterodimer through backbone-backbone interactions. Angew.Chem.Int.Ed., **44**, 5710-5713 **(2005)**.

[31] C.Gailer, M.Feigel; Is the parallel or antiparallel β-sheet more stable? A semiempirical study. J.computer-Aided Molecular Design, **11**, 276 **(1997)**.

[32] W.G.Hoover; Canonical dynamics: equilibrium phase-space distributions, Phys.Rev.A., **31**, 1695-1697 **(1985)**.

[33] H.Sun; Ab Initio Calculations and Force Field Development for Computer Simulation of Polysilanes, Macromolecules, **28**, 701-712 **(1995)**.

[34] H.Sun; COMPASS: An ab initio force-field optimized for condensed-phase applications—overview with details on alkane and benzene compounds, J.Phys.Chem.B., **102**, 7338-7364 **(1998)**.

[35] H.Sun, P.Ren, J.R.Fried; The COMPASS Force Field: Parameterization and Validation for Polyphosphazenes.Comput.Theor.Polym.Sci, **8**, 229-246 **(1998)**.

[36] R.Garcia-Fandino, L.Castedo, J.R. Granja; Interaction and Dimerization Energies in Methyl-Blocked α,γ-Peptide Nanotube Segments. J.Phys.Chem.B.,

114, 4973-4983 **(2010)**.

[37] R.Garcia-Fandino, J.R.Granja, M.DAbramo; Theoretical Characterization of the Dynamical Behavior and Transport Properties of α,γ-Peptide Nanotubes in Solution. J.AM.CHEM.SOC., **9(131)**, 15678-15686 **(2009)**.

[38] J.Cheng, J.C.Zhu, B.Liu; Molecular modeling investigation of adsorption of self-assembled peptide nanotube of cyclo-[(1R,3S)-γ-Acc-D-Phe]$_3$ in $CHCl_3$. Chem.Phys., **333**, 105-111 **(2007)**.

[39] J.Liu, J.F.Fan, M.Tang, W.Q.Zhou; Molecular Dynamics Simulation for the Structure of the Water Chain in a Transmembrane Peptide Nanotube. J.Phys.Chem.A., **114**, 2376-2383 **(2010)**.

[40] H.W.Tan, W.W.Qu, G.J.Chen, R.Z.Liu; Theoretical investigation of the self-assembly of cyclo[(-β^3-HGly)$_4$-]. Chem.Phys.Lett., **369(5-6)**, 556-562 **(2003).**